1ˢᵗ Edition

FabSpace Use Cases Series

May 2018

Contents

1. Introduction

The 1st edition of the FabSpace Use Cases Series is part of the initiative **FabSpace 2.0 (https://www.fabspace.eu/)**, a project funded by the European Union Horizon 2020 Programme (H2020). The project aims at making universities open innovation centres for their region and improving their contribution to the performance of societies. It will concentrate on one innovation area with high expected socio-economic and environmental impact: geodata-driven innovation, by leveraging space data in particular.

Specifically, this Use Cases series is part of the activities foreseen within work package **(WP) 4 - Exploitation and dissemination**, which are implemented throughout the entire lifetime of the project.

WP4 is the central WP for the Exploit, sustain and disseminate the FabSpace concept by:

1) Demonstrating the financial sustainability of this new university service and understanding the culture and potentially conflicting objectives of the partners involved;
2) Expanding the concept into new universities in Europe and worldwide; and
3) Creating an international network to consolidate final user needs and industry requirements.

This document presents the 1st edition of collected use case implemented by FabSpace partners.

This edition is thus structured in the following central sections:

- Section 2: **"Use Case 1: Epidemic Disease Mapping in Africa"** – this section includes the use case developed by FabSpace Darmstadt, Germany in collaboration with Merck and ESOC at Darmstadt;

- Section 3: "**Use Case 2: Implementation of Earth Observation image processing via Neural Networks on Embedded Architectures**" – this section includes the use case developed by FabSpace Greece;

- Section 4: "**Use Case 3: Regional Population Estimation Using Satellite Imagery**" – this section includes the use case developed by FabSpace Greece;

- Section 5: "**Use Case 4: Hyperspectral Earth Observation Image Processing On FPGAs**" – this section includes the use case developed by FabSpace Greece;

- Section 6: "**Use Case 5: Calculation of damage in forests using Sentinel-2**" – this section includes the use case developed by FabSpace Warsaw, Poland;

- Section 7: "**Use Case 6: Mapping deforestation in a location of interest**" – this section includes the use case developed by FabSpace Toulouse, France;

- Section 8: **"Use case 7: "Global Warming impact assessment on the Bracciano Lake Surface Temperature"** – this section includes the use case developed by FabSpace Rome, Italy.

The next edition of the use cases implemented within FabSpace partners shall be published regularly during the entire lifetime of the project.

Use Case 1:

Epidemic Disease Mapping in Africa

Implemented by: FabSpace Darmstadt, Germany

Contact: **Md Bayzidul Islam** (*bislam@psg.tu-darmstadt.de*)

2. Use Case 1: Epidemic Disease Mapping in Africa

Recently in the Innovation Action Event organized by the FabSpace Darmstadt in collaboration with Merck and ESOC at Darmstadt where the use case has been created. The ideation and detailed case was developed in collaboration with Merck and FabSpace experts. In the event Sentinel Hub was supported by giving enterprise access to their data platform where the pre-process of satellite imagery was conducted and collected afterwards for further processing.

The objective of the work was how to track the spread of neglected tropical diseases - NTDs from space? In the current case it was determined to focus on the African Trypanosomiasis (sleeping sickness) as the epidemic disease. The goal was set to create a first version of geo-located model describing which areas are prone to be affected. Moreover, it was also determined that what are the probable factors that are allowing flies to spread and consequently what can be measure with the available satellite data.

According to the state of the art, it is found that the Tsetse fly is the vector of the disease and thus it is fundamental to identify the suitable living and growing conditions satisfying locations of those flies. Therefore, some parameters were defined on the Tsetse fly that has to be identified by using the available Earth Observation Satellite Sentinel-2 data. Those parameters are considered as, a) Living conditions b) Predict vulnerable areas and c) Predict the spread of the insect.

Description:

Using Earth Observation data, how to identify:

➢ Areas which are prone/susceptible for the spread of African Trypanosomiasis, also known as Sleeping Sickness
➢ It is caused by the Tsetse fly as an insect and what risk factors that allow the spread of this fly
➢ By using EO data, how to determine possible cause that increase to spread. What is the benefit of incorporating other weather data for the DR Congo (Kinshasa city)
➢ Validate it for Kinshasa, DR Kongo area

Human African Trypanosomiasis (sleeping sickness)

➢ Sleeping sickness occurs in 36 sub-Saharan African countries and around 70 million people are at risk

➢ The people most exposed to disease live in rural areas and depends on agriculture, fishing, animal husbandry or hunting

➢ The risk factors of the vector (Tsetse Fly) growth are average temperature, above 38 Deg.C and below 15 Deg.C is not suitable

➢ In general marshland and watery area with vegetation cover where there is average temperature is more suitable for normal growth of this insect

Distribution of human African Trypanosomiasis

From the literature it is found that the DR Kongo has the strongest spread of the disease in 2010 and it is continuing year after year. It is also found that the city Kinshasa is the most affected area and it is meaningful to take the city as a study area.
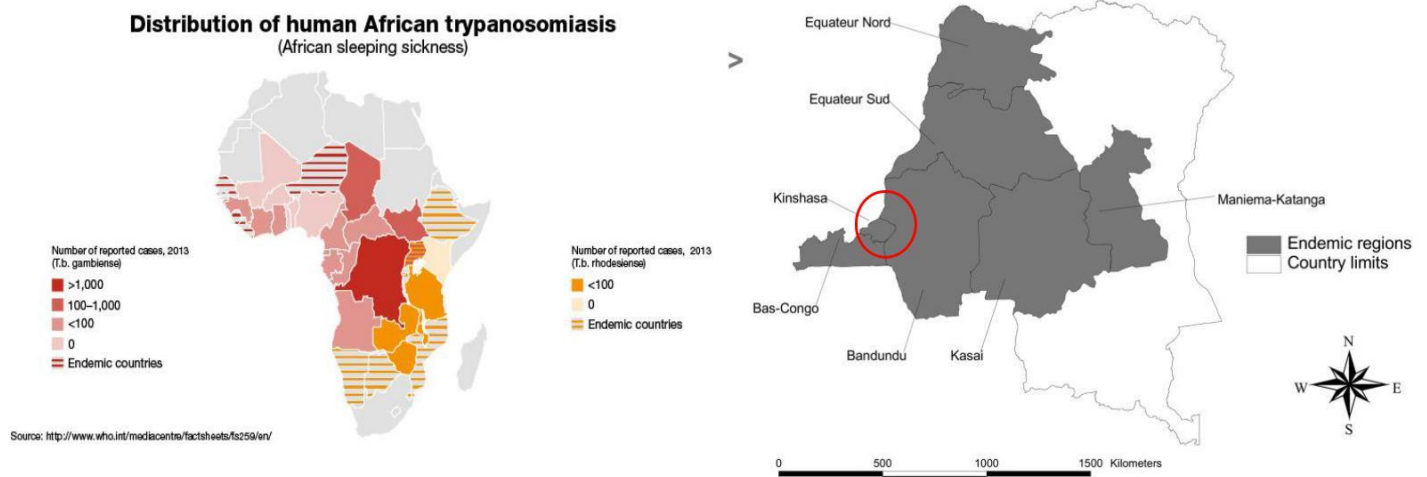

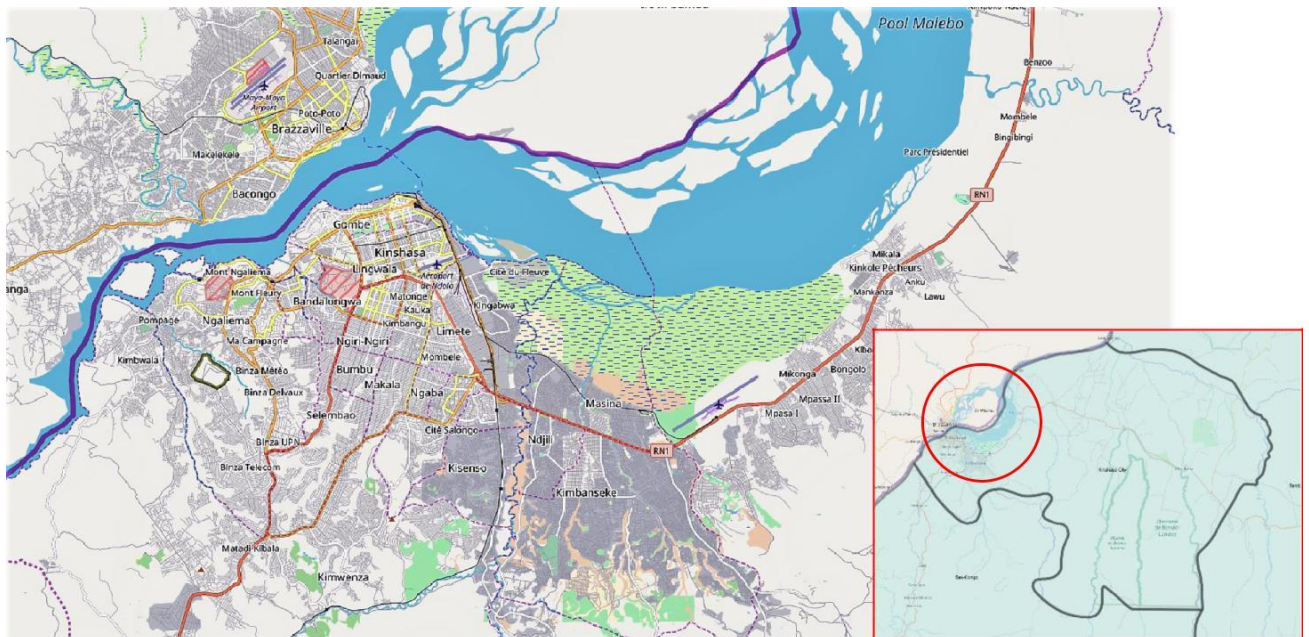**Fig-1**: Selected Region Kinshasa City

Fig-2: Get to know the area using google street map as an overlay. Basic visual understanding of the area using google street map

Image Processing:

Satellite image gives the opportunity to create the true color map of the area as follows. The raw true color images are not always easy to interpret for any specific purpose and thus needs to process using programing interface or any desktop based software like SNAP or QGIS to explore which we cannot see through the necked eyes.
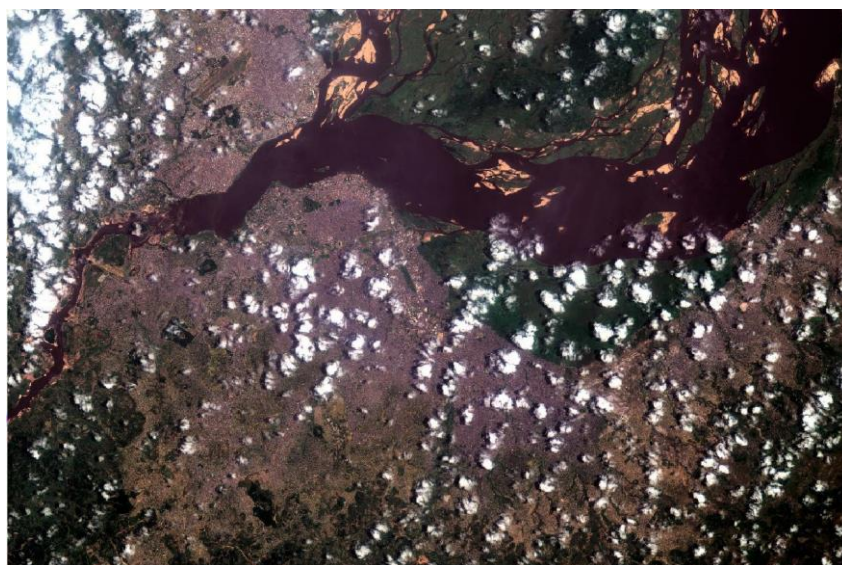

Fig-3: True color Image, March 2017 (Source: data from Sentinel Hub / ESA)

In the previous true color satellite image, we can see all the noise and cloud which is not clear to assess the area visually and therefore, there is promising functionalities to represent the image in false color to make it more visible as follows. In the false color image green is showing vegetation, water bodies are appearing as blackish and the violet color is representing the settlements where yellowish color represents bare soil.

Fig-4: False color Image, March 2017 (Source: data from Sentinel Hub / ESA)

Now if we deep dive into the analysis then firstly the Normalized Difference Vegetation Index (NDVI) is a simple graphical indicator that can be used to analyze the land type characteristics of the area as segmenting green vegetation and other types. The NDVI index can help to completely segment the settlement area and the vegetation cover as clear as possible. The land segments which covered fully or partly by vegetation resulting from the NDVI is suitable condition to live and grow the insect.
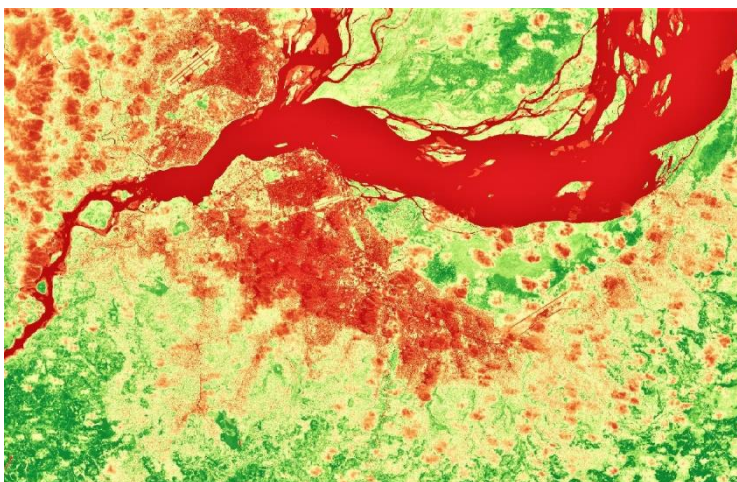

Fig-5: NDVI Image, March 2017 (Source: data from Sentinel Hub / ESA)

In the next possible step, it is logical to identify the area contains water or marshland. The simple Normalized Difference Water Index (NDWI) can be used to segment the area based on water and other uses. Although the cloud has not been extracted here but normalized in the next process.
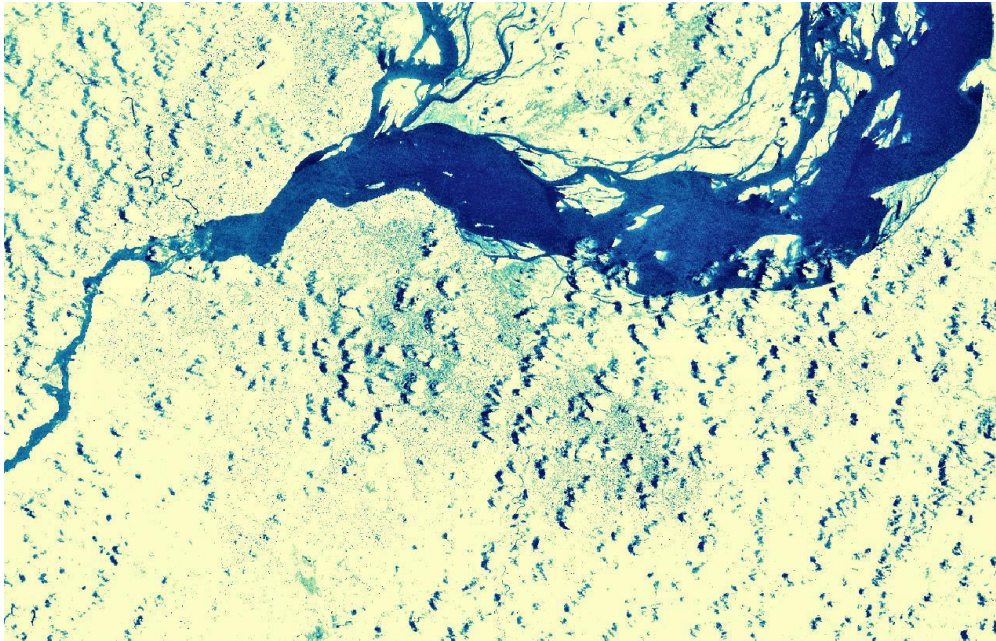

Fig-6: NDWI Image (Blue indicates water), March 2017 (Source: data from Sentinel Hub / ESA)

The third parameter is the temperature which denotes that if there is an average temperature that creates the suitable living environment for the insects. In this regard identifying temperature map leads to consider soil moisture map of two different seasons as rainy and dry. It is evident that when there is high moisture content, naturally in rainy season indicates low temperature and the low moisture content in the dry season is a clear indication of the opposite higher temperature. Therefore, the average of this two moisture map of two seasons can fundamentally help us to identify suitable dry or wet location for the insect to live and grow.

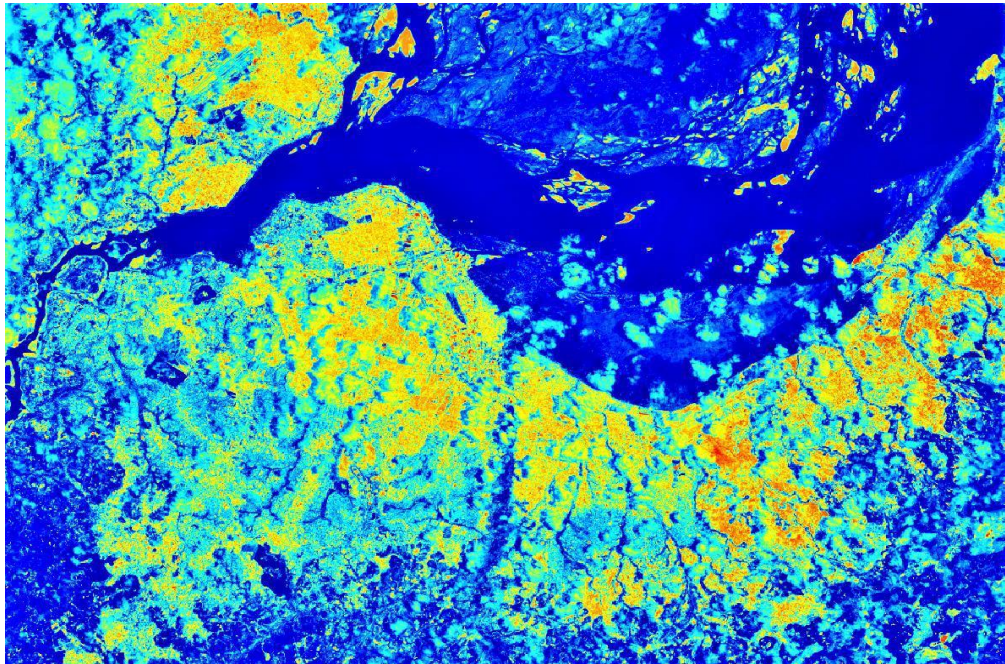**Fig-7**: Soil Moisture Index (dark to light color indicates high to low value) in Rainy Season Feb-March 2017 (Source: data from Sentinel Hub / ESA)
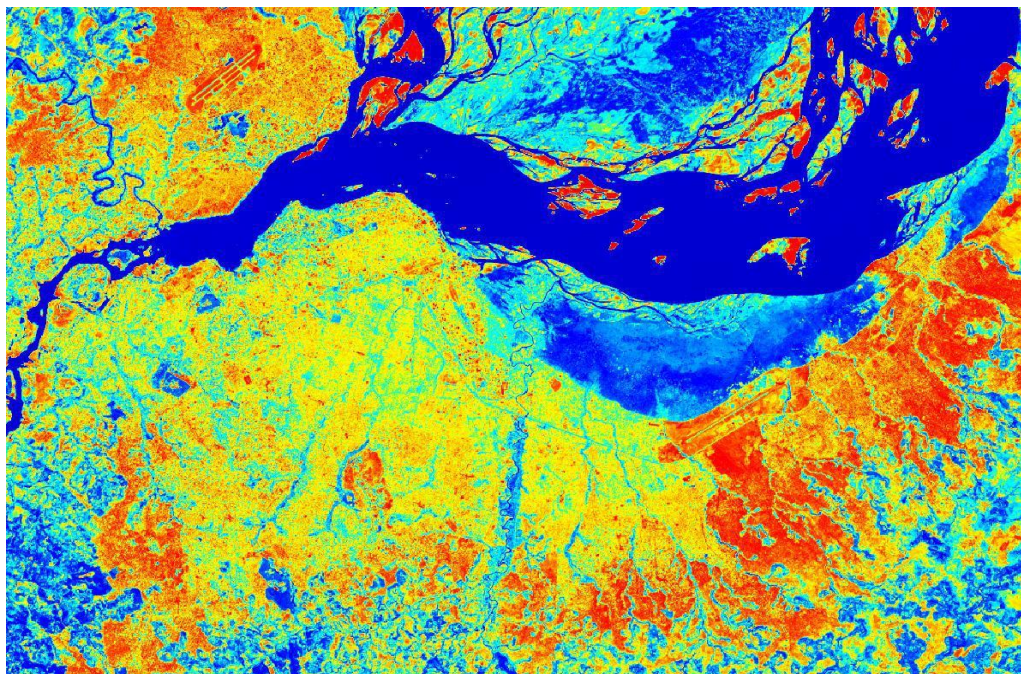

Fig-8: Soil Moisture Index in dry Season June-July 2017 (Source: data from Sentinel Hub / ESA)

In the conclusion, when we have the map of all three parameters (vegetation, water and temperature) and all the raster maps containing value in binary fission as 0 and 1 according to the importance. Then we can easily cross correlate all three maps where we will get only the value 1 which is true for each case. At the end of the day we could have our desired geo-located map of vulnerable areas which meets all the three criteria. It is explored that the Kinshasa city is expanding outer wards and in contrary the flies are moving towards the city. Therefore, the vector of the disease is moving towards the inhabitants while the inhabitants are also creating situation to spread the disease in an epidemic manner.
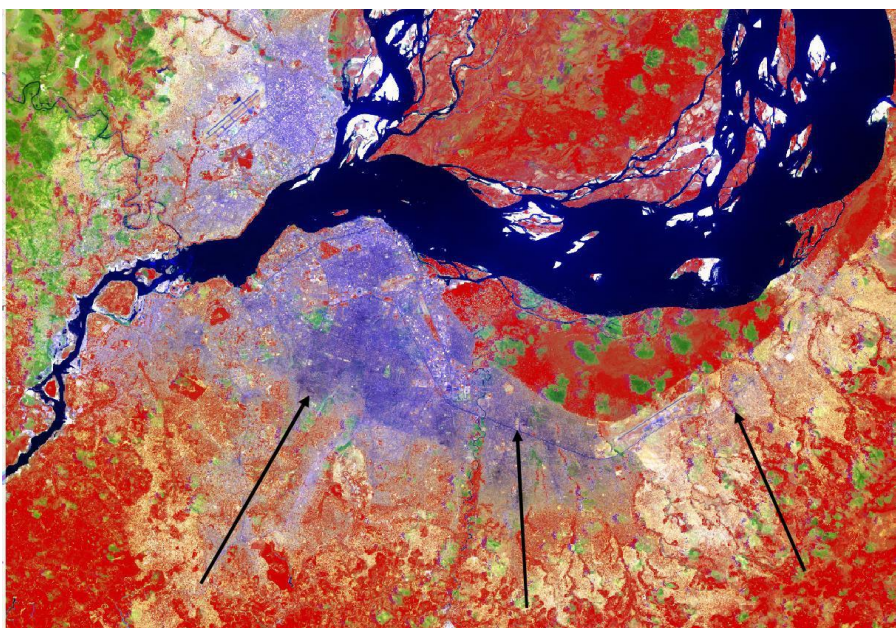
Fig-9: Result of the study as vulnerability map (Red color shows suitable locations)

Fig-10: Result of the study as vulnerability map showing suitable location inside the Kinshasa city

Use Case 2:

Implementation of Earth Observation image

processing via Neural Networks on Embedded Architectures

Implemented by: FabSpace Greece

Contact: Iosif S. Paraskevas (*isparas@mail.ntua.gr*) &
Haris Marantos (*hmarantos@microlab.ntua.gr*)

3. Use Case 2: Implementation of Earth Observation image processing via Neural Networks on Embedded Architectures

During a Diploma Thesis [1] in School of Electrical and Computer Engineering in National Technical University of Athens the present use-case has been created.

Disciplines involved:

- Computer engineering

- Machine Learning

- Image Processing

- Remote Sensing

Introduction:

In recent years, the processing of Earth Observation images has an increasing number of applications in areas of geology, agriculture, surveillance and physics, such as environmental monitoring, food processing, high speed sensing etc.

Using machine learning techniques tends to be a very efficient way to recognize specific places and objects in Earth Observation images. Artificial Neural Networks, which are biologically inspired computational models, exceed a spectacular performance for a lot of image recognition tasks.

In order to achieve high accuracy in processing EO images, machine learning methods turn out to be computationally intensive leading to large time delays and high energy consumption, creating problems for embedded devices. In this direction optimizations both in techniques/ software and in hardware systems are applied.

In this use-case, an efficient EO image recognition via Neural Networks was applied, in terms of performance, execution time and power dissipation, on an ultra-low-power System on Chip, namely the Intel Movidius Myriad 2.

Tools and Platforms:

Myriad 2 is a multi-processor System on Chip (SoC), which provides low-power, high-performance vision processing solutions. It incorporates 2 LEON 32-bit processors. The first one is responsible for the communication with the outside world, controlling all the external peripherals and runs a simple operating system, while the second one, controls the media devices. Additionally, Myriad 2 includes

12 SHAVE (Streaming Hybrid Architecture Vector Engine) processors. These contain Very Long Instruction Word (VLIW) architecture, supporting 128-bit operations in one clock cycle, for supporting high parallelism and throughput. Moreover, Myriad 2 includes a software-controlled memory subsystem, called Connection Matrix (CMX). Figure 1 illustrates the block diagram of Intel Movidius Myriad 2 [2]. Figure 2 shows the development board that was used in this use-case.

Figure 1. Intel/ Movidius Myriad 2 detailed block diagram.

Figure 2. Myriad™ Development Kit & Board
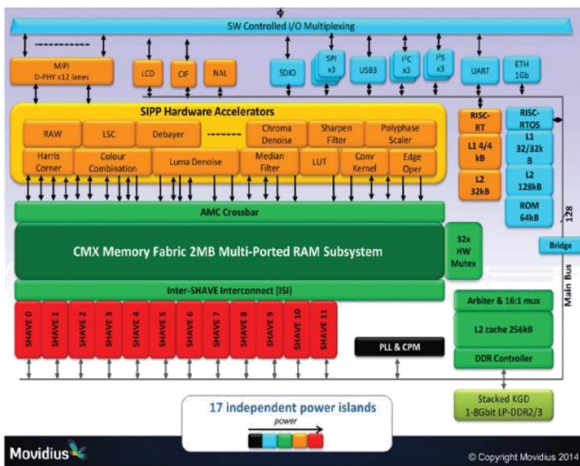
Methods:

Convolutional Neural Networks (CNN) were used for recognizing buildings, trees, barren land, grassland, road and water. CNNs are a subcategory of ANNs that are very efficient in computer vision and image recognition problems. Figure 3 depicts an example of the CNN topology.
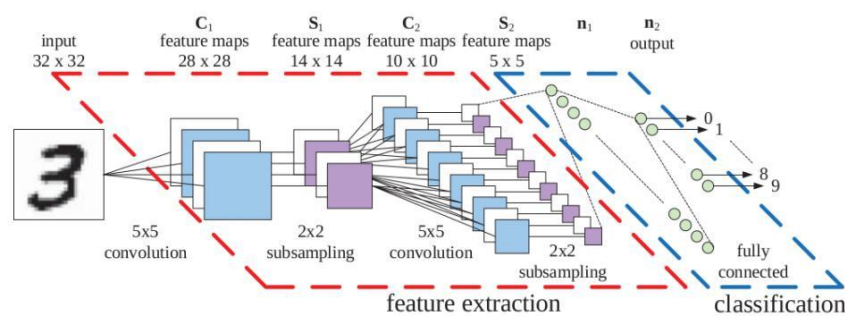

Figure 3. Example of CNN topology.

Applied optimizations:

- Efficient exploitation of CMX memory: The code that SHAVEs execute is transferred to DRAM (DDR and cache memory maintain the performance, while CMX gains up to 50% more space)

- New strategy for minimizing data transfer between DDR and CMX (changes in nested loops in order to use the same input volume for generating more output maps)

- Double buffering for DMAs engine

- Function calls reduction (Because Myriad 2 has not a branch prediction mechanism)

- Reduction of the numerical precision to 16bit for high parallelism

Results:

The efficient implementation of CNNs in Myriad 2 leads to similar results to the *Caffe* suite [3] running on Intel Xeon E5-2650 CPU for recognizing buildings, trees, grassland, barren land, road and water in Earth Observation images but with significant energy savings. Additionally, the proposed implementation achieves lower execution time than Intel Neural Compute stick that is specified for this kind of applications.

References:

[1] Xygis Athanasios, Implementation of Convolutional Neural Networks on Embedded Architectures, 2017, Diploma Thesis NTUA

[2] D. Moloney, B. Barry, R. Richmond, F. Connor, C. Brick, and D. Donohoe, "Myriad 2: Eye of the computational vision storm," in IEEE Hot Chips Symposium (HCS), Aug. 2014, pp. 1–18.

[3] Y. Jia, E. Shelhamer, J. Donahue, S. Karayev, J. Long, R. Girshick, S. Guadarrama και T. Darrell. Caffe: Convolutional Architecture for Fast Feature Embedding. ArXiv e-prints, 2014.

Use Case 3:

Regional Population Estimation Using Satellite Imagery

Implemented by: FabSpace Greece

Contact: Iosif S. Paraskevas *(isparas@mail.ntua.gr) &*
Haris Marantos *(hmarantos@microlab.ntua.gr)*

4. Use Case 3: Regional Population Estimation Using Satellite Imagery

Overview

Recently in the HackOnEarth hackathon co-organized by the FabSpace Greece and Corallia in Athens Sentinel Hub gave enterprise access to their data platform where the pre-process of satellite imagery was conducted and collected afterwards for further processing in order to remotely estimate population in areas of Uganda and Zambia.

Description

The work is directed at the automated estimation of population using Supervised Classification through a GIS platform applied to satellite imagery. The motivation for the work is that the collection of population data, when conducted in the traditional manner can be time consuming and inefficient. This is especially the case in rural areas that lack of sophisticated communication and transport infrastructure, especially in developing countries. The solution proposed in this paper is based on the concept of using satellite imagery in order to estimate the population. The concept includes using a small sample of satellite images to build a classifier that can then be used to predict populated areas. The main issue to be addressed is how to best use the classified result towards matching it to the number of people in the study area. In order to correspond to the task described above, the following methodology is proposing (i) an image supervised classification technique , (ii) a statistical forecasting procedure and (iii) a regional disaggregation technique.

Classification

The input data consists of polygon shape-files, composed of points that determine the border of the areas of interest. Through the geographic information system (in our case, QGIS) we use the polygon shapes as an input, we define the parameters (desired date of acquisition, cloud coverage etc.) and download the image files.
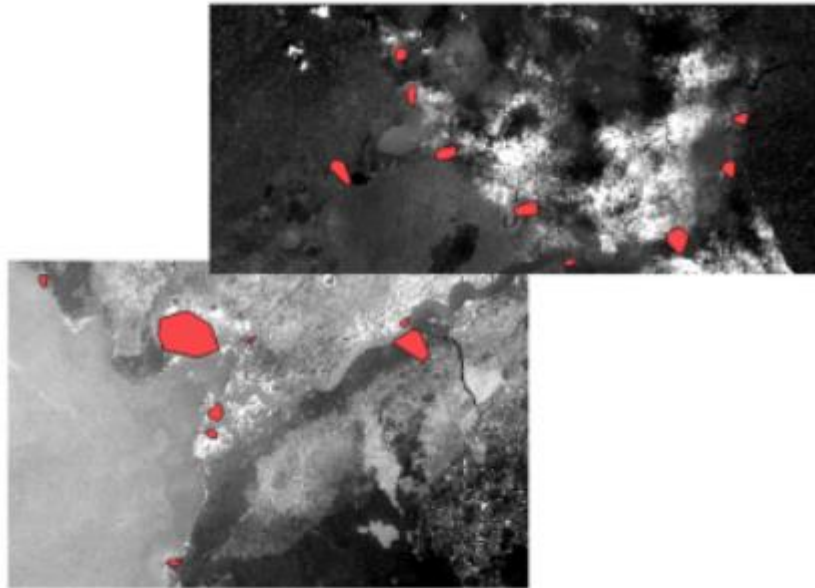
In order to make use of the multitude of digital data available from satellite imagery, it must be processed in a manner that is suitable for the end user. For many projects this processing includes categorizing the land into its various use functions (for example extracting 3 different categories, water, grass and buildings). In the case of supervised land classification, the individual processing the imagery guides the image processing software to help it decide how to classify certain features. This is done by the use of a vector layer containing training polygons.

After the image processing is completed we are left with a 2-color pixelated high resolution picture, with white representing the buildings of the specific area and black representing the non-living areas.

Statistical Forecast

On those extracted pictures, we need to determine a population density multiplier for each pixel. After producing forecasts for the total population we have to attempt a regional disaggregation based on that individual data we have access to. We perform a cross-validation competition between several methods including MAPA, ETS, Theta, ARIMA, SES, Holt, and Damped through the OMEN platform. The best fitted model is selected which in this case was the ARIMA model. Through this forecast we calculate the density multiplier for the different regions.

In conclusion, the clipped pixelated images along with the multipliers can be used as input to calculate the population of each region. For each compound, each white pixel is multiplied by the estimated weight variable of the respective study area (11.5834 for Uganda - 7.02352 for Lusaka). The outputs provide with the final dataset containing the population estimations for all the subregions of each country.

Use Case 4:

Hyperspectral Earth Observation Image Processing On FPGAS

Implemented by: FabSpace Greece

Contact: Iosif S. Paraskevas (*isparas@mail.ntua.gr*) &
Haris Marantos (*hmarantos@microlab.ntua.gr*)

5. Use Case 4: Hyperspectral Earth Observation Image Processing On FPGAs

During a Diploma Thesis [1] in School of Electrical and Computer Engineering in National Technical University of Athens, the present use-case has been created. A scientific publication in IEEE International Symposium on Circuits & Systems 2017, regarding this use-case was submitted and presented [2].

Disciplines involved:

- Computer engineering

- Image Processing

- Remote Sensing

Introduction:

In recent years, the processing of Earth Observation hyperspectral images has an increasing number of applications in areas of geology, agriculture, surveillance and physics, such as environmental monitoring, food processing, high speed sensing etc. The accuracy, the time delay and the energy that is consumed for processing this kind of images are very important parameters. In this direction, optimizations on processing both in techniques/ software and in hardware systems are applied. Field Programmable Gate Arrays (FPGAs) are commonly used devices that offer increasing computational performance, due to their high parallelization and reconfiguration ability.

In this use-case it was examined how effective could be the use of FPGAs and how much can increase the process of large amount of data simultaneously achieving near real time response. The accelerated system matches incoming pixels from hyperspectral cameras with a set of spectral signatures known a priori and is used in order to recognize specific places and objects (water, courts, field, trees etc).

Data:

The main dataset was composed by Earth Observation hyperspectral images (from APEX - Airborne Prism Experiment), depicted in Figure 1, as well as images from objects captured by hyperspectral cameras (by the Remote Sensing Laboratory of the NTUA), an example of which is illustrated (in true color) in Figure 2, as color references.

Fig. 1. True Color Earth Observation Image   **Fig.2**. Reference (by NTUA Remote Sensing Lab)

Tools and Platforms:

FPGAs are semiconductor devices that include configurable logic blocks, memories, embedded functions and offer flexibility and very fast processing capabilities. FPGAs can achieve near real-time response, especially in application such as in this case, which have computational characteristics. Furthermore, FPGAs are very energy efficient, something that it is very important when the processing is operated in embedded devices (for example UAVs, which is a modern Earth Observation platform that is used in a huge range of applications nowadays).

Methods:

The methods that were examined and implemented in this use-case were the parallelization of pixel-by-pixel matching for 3 different matching kernels.

Hardware architecture was developed parallelized at 3 distinct levels:

- Pixel (process multiple pixels at the same time)

- Signature (compare 1 pixel to multiple signatures simultaneously)

- Channel (multiple partial sums concurrently)

Results:

The example objects that were recognized are noted in Figure 3. The proposed HW architecture (implemented in a Zynq-7000 SoC) achieved around 97%, 75%, 45% and 88% accuracy for recognizing water, soccer-fields, trees and courts respectively providing an acceleration of 40−355x vs Intel-i3 CPU and 360−10^4x compared to the embedded ARM Cortex A9 CPU.

Fig.3 Example objects (water, courts, field, trees)

More information and details:

[1] S. Vellas, Parallel Architecture Design And Trade-off Analysis For Hyperspectral Image Processing On Fpga, Diploma Thesis ECE NTUA

[2] Vellas, Simon, et al. "FPGA acceleration of hyperspectral image processing for high-speed detection applications." Circuits and Systems (ISCAS), 2017 IEEE International Symposium on. IEEE, 2017.

Use Case 5:

Calculation of damage in forests using Sentinel-2

Implemented by: FabSpace Warsaw, Poland

Contact: Paulina Sciana (_paulina.sciana@opegieka.pl_)

# 6. Use Case 5: Calculation of damage in forests using Sentinel-2

During the Daily Animation organized by FabSpace Warsaw, people registered for the course "Sentinel-2 on the example of defining damage in the forests", could learn to work with Senitnel-2, perform supervised classification and thereby determine the area of destruction in the forests.

Workshops have been developed by FabSpace experts. The purpose of the work was to determine the area of damage in the area of two forest districts in Poland: Czersk and Rytel Forest Districts. The destruction was caused by the strong storms at night from 11 to 12 August 2017 through the western part of Poland. Damage was reported in about 60 regional forest districts, the workshops were prepared for two, where losses were one of the largest.

Losses estimated by Polish forestry agency - Poland State Forests are 9,8 million m3 fallen and broken trees, 79,7 thousand ha of damaged forests, including 39,2 thousand ha for total renovation.

Two Senitnel-2 imagery from Copernicus Open Access Hub were used in the work. Satellite images came from before the storm: 01/05/2017 and after the storm: 28/09/2017. The .shp vector layers of the Czersk Forest District and the Rytel Forestry District were also used.

The work was carried out in open QGIS software with the Semi-Automatic Classification Plugin.
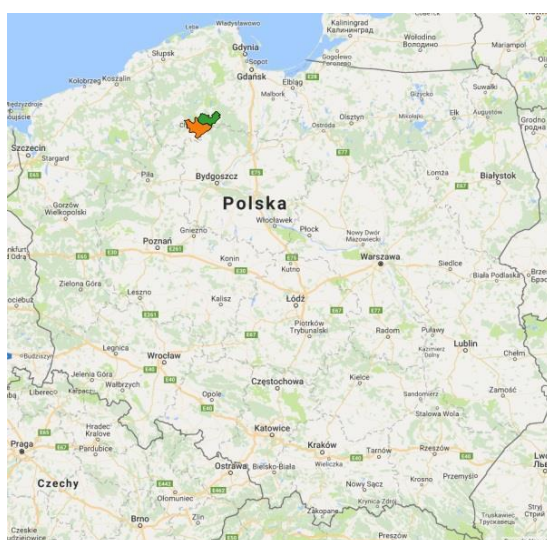
Areas of the Czersk and Rytel forest districts (green - district Czersk, orange - district Rytel)

The main problem in Poland and the use of multispectral data, for example Senitnel-2, is high cloud cover in Poland during the year. For destruction in forests from 11-12 August, cloudless data after damage was only available from 28 September.

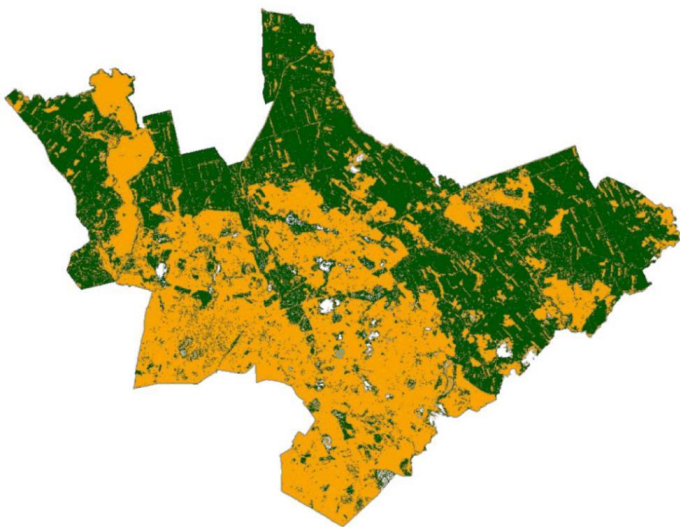*Research area from Sentinel-2 RGB 01.05.2017*
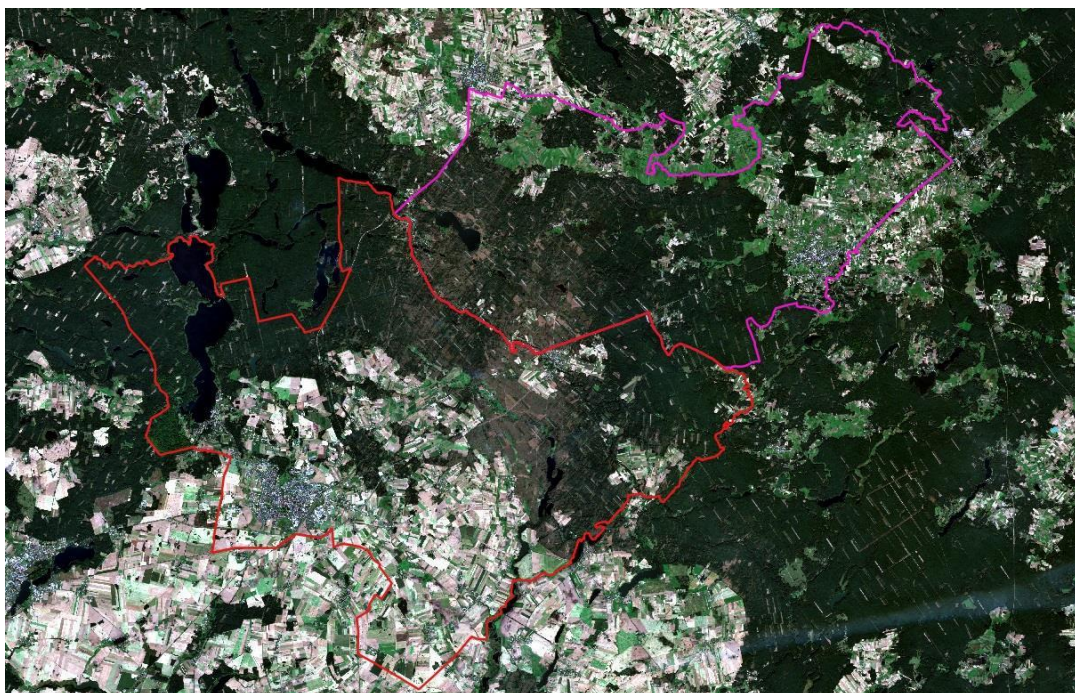
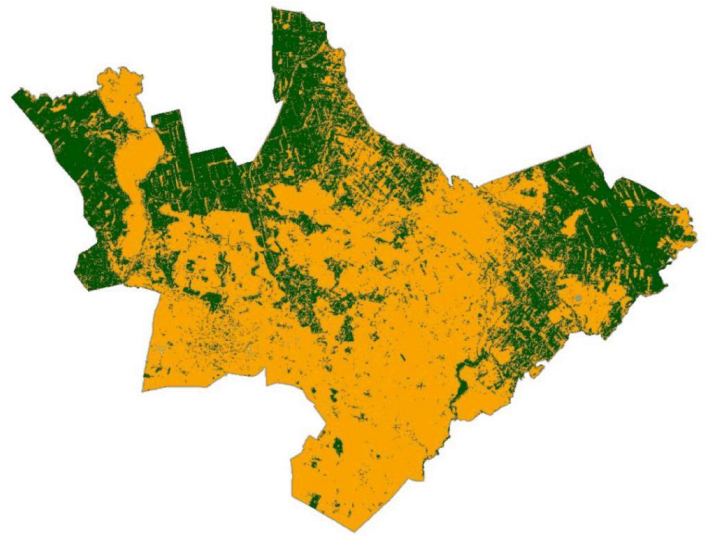*Research area from Sentinel-2 RGB 28.09.2017*

Area Rytel Forest District from 01.05.2017,

Senitnel-2 RGB

Area Rytel Forest District from 28.09.2017,

Senitnel-2 RGB

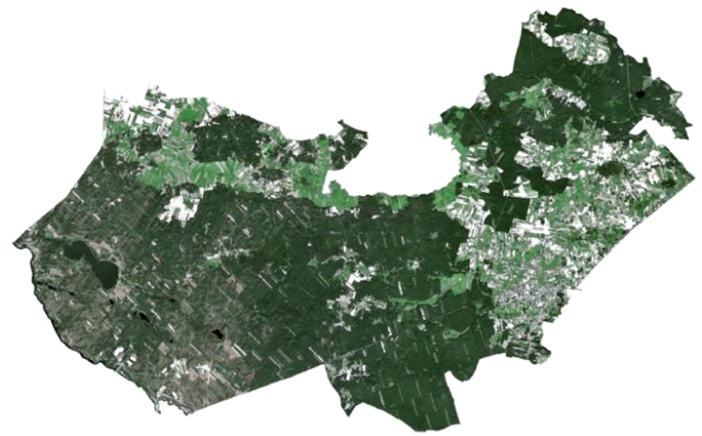*Classified area Rytel Forest District from*

01.05.2017

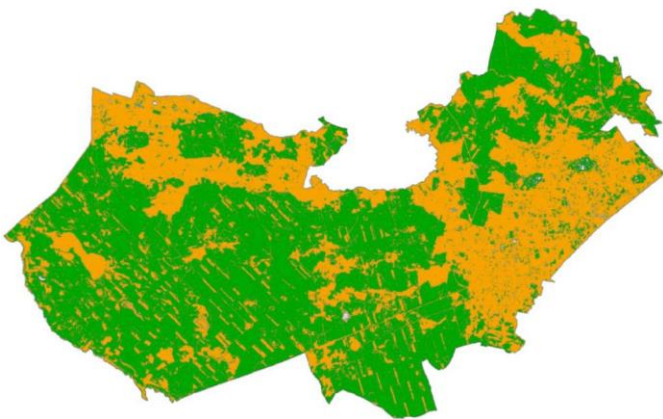*Classified area Rytel Forest District from*

28.09.2017

Steps:

- Downloading images after atmospheric correction (Level 2A) from the service: https://scihub.copernicus.eu/dhus/#/home,

- To limit the classification results only to Rytel and Czersk Forest District, satellite images have been cut off by the .shp vector layer of both Forest Districts,

- Supervised classification for images from both months into two classes: "forest" and "others". The separation of only two classes was to serve only the purposes of visualization. Coverage changes for May and September were also visible on crop fields, due to vegetation in May and plowing fields in September. Coverage changes could false point to a larger area of damage. The division into two classes eliminated this problem.

- Supervised classification was made using the maximum likelihood.

- Determination of the difference in forest area from May and September on the basis of the classification report - the difference is destroyed forest area.
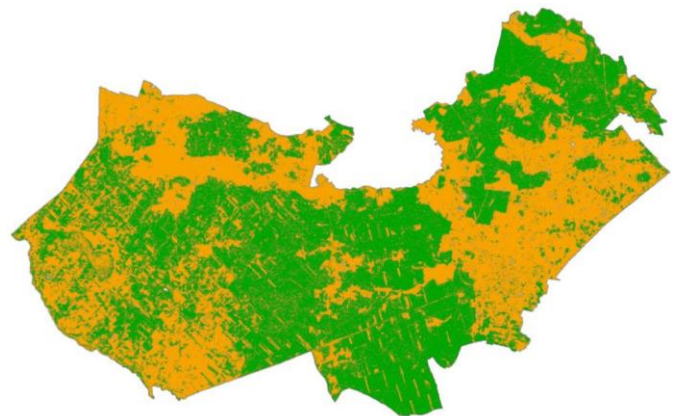
Area Rytel Forest District from 01.05.2017,

Senitnel-2 RGB

Area Rytel Forest District from 01.05.2017,

Senitnel-2 RGB

Classified area Czersk Forest District from

01.05.2017

Classified area Czersk Forest District from

28.09.2017

	Area [ha]	%	Area [ha]	%
	Forest District Rytel		**Forest District Czersk**	
May	17341,56	46,6	15474,44	57,8
Semtember	12659,93	33,6	12776,69	47,6
Difference	**4681,63**	**13,0**	**2697,75**	**10,2**

Summarize the results of the classification and determining the forest area before the storm and after the storm. For the Rytel Forest District, the area of destroyed forests is 4681,63 hectares, which constitutes **13%** of the area of this forest inspectorate. In the case of Czersk Forest District, it is 2697,75 ha, which is **10,2%** of the whole forest inspectorate.

To sum up, the Sentinel-2 mission fulfills its goals, but in the case of heavily clouded areas like Poland, sometimes we have to wait longer for these data.

Use Case 6:

Mapping deforestation in a location of interest

Implemented by: FabSpace Toulouse, France

Contact: Nathalie Neptune (*nathalie.neptune@irit.fr*) &
Laure Vacquié (*laure.vacquie@irit.fr*)

7. Use Case 6: Mapping deforestation in a location of interest

The large quantity of satellite imagery available for free makes it possible to track different geo-phenomena in locations of interest all over the earth. In the case of deforestation, previous work has been done to produce a global map of forest cover change from the year 2000 to 2012 (Hansen, et al., 2013). Taking Madagascar as an example, the loss/gain of tree cover can be seen on a map generated using the time-series analysis of Landsat images done by Hansen et al. (Hansen, et al., 2013) with data from 2000 to 2014. The forest cover in 2000 is shown in green and the forest loss is shown in red and the forest gain is in blue.
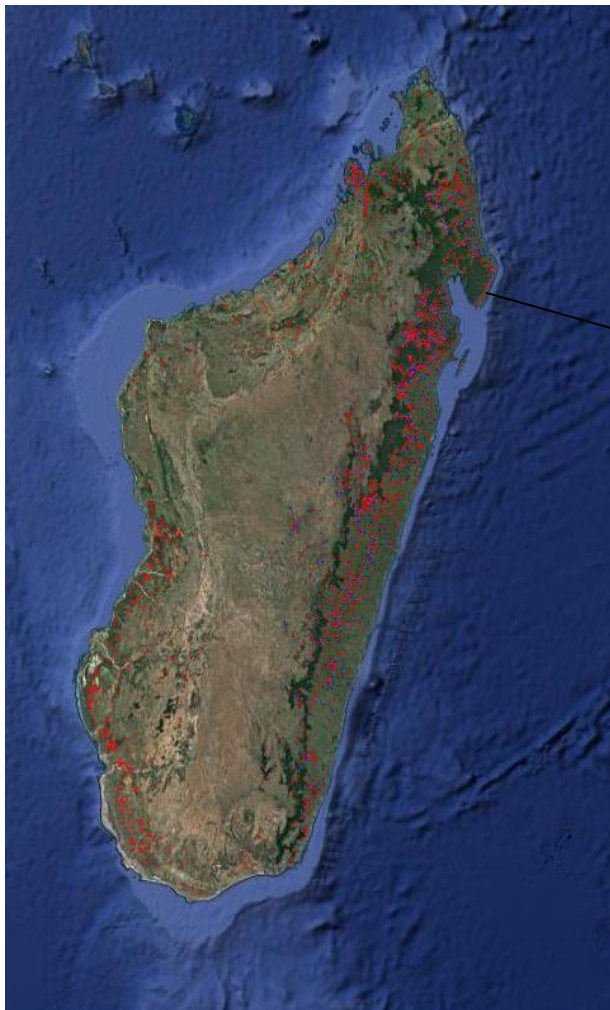

Figure 1. Forest cover loss and gain in Madagascar from the global forest change map – Image source: Google Earth Engine
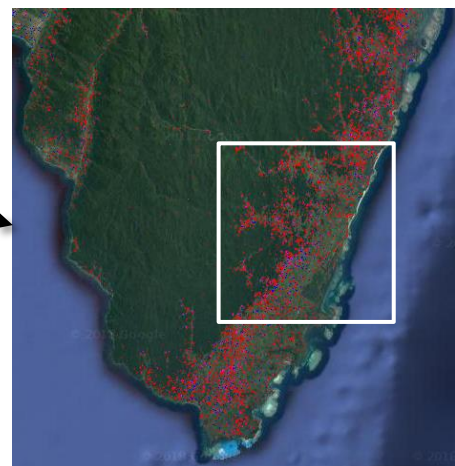

Figure 2. Enlarged image of the coastal area in the north east of the island of Madagascar near Masoala park – Image source: Google Earth Engine

Combining radar and optical satellite images for deforestation detection

The Copernicus program through its Sentinel-1 radar imagery and Sentinel-2 optical imagery allows the possibility of better forest mapping by combining these two types of images. In this way, more precise change maps can be produced to follow the evolution of forests over time and see to what extent they are being affected by deforestation. The workflow below shows the steps to using Sentinel-1 radar imagery and Sentinel-2 optical imagery to produce a change map. This process can be applied for deforestation and other changes that can be detected with earth observation images.
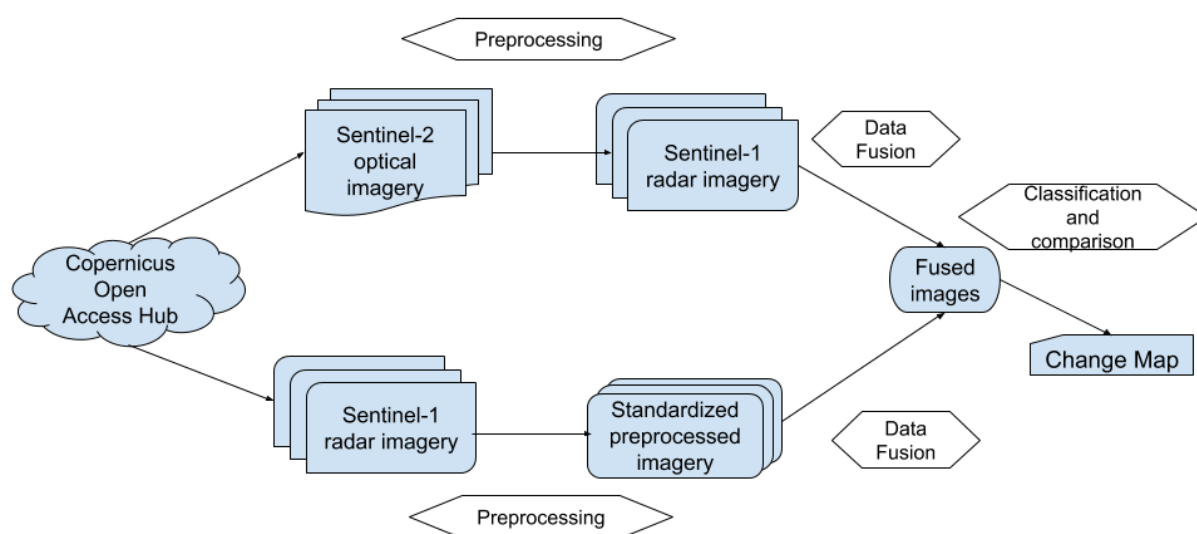
Figure 3. Workflow for Combining Sentinel-1 and Sentinel-2 Data for Change Detection

Forest mapping example

This example is done using ESA's SNAP – Sentinels Application Platform.

One sentinel-1 image and one sentinel-2 image covering the area highlighted in figure 2 and from the same period (February 18-20, 2017) were downloaded. We can view both images with the resulting fused image in table 1.

The sentinel-2 image for February 20th, 2017, is shown in natural colors. This image was chosen because it includes a large part of forest-covered area and presents very little cloud cover. The image is then resampled and reprojected to have the coordinates in latitude and longitude (WGS 84).

The laser image for February 18th, 2017, is shown using the Dual Pol Difference Sigma0 db VV + VH option. This image was chosen because it is the closest one to the date of the optical image available for the same area. Typical processing for radar images was done: calibration, speckle filtering, terrain correction and db conversion.

A subset of each image is created using the coordinates of the area of interest. The fusion of these two subsets is done by creating a stack using the stacking option in SNAP. The resulting stack contains both the sentinel-1 and sentinel-2 information.

Vector data geometries are created on each image for training the classifier that will later be used to classify the entire image. These shapes are classified manually by visual interpretation. Eight classes were defined; their names and assigned colors are listed in table 2.

Using a k-nearest neighbors (KNN) classifier on each image, we get the resulting classified images. KNN is a simple supervised machine learning algorithm; it classifies elements based on their distance to the nearest known sample. The color and label for each class are given in table 3.

By visually examining the resulting classifications, we can see that the classification of the fused image gives a more complete picture of the tree covered areas compared to the classification of the sentinel-2 image alone while the result from the sentinel-1 image classification appears to be very noisy.
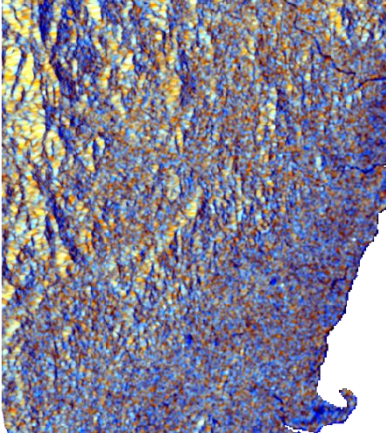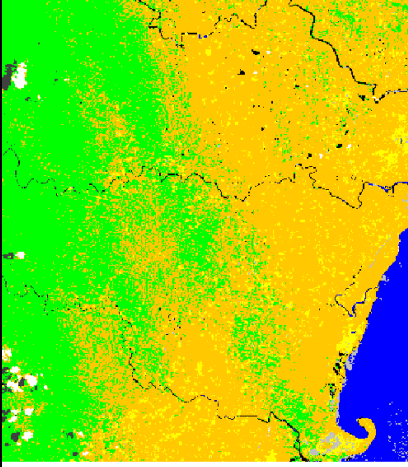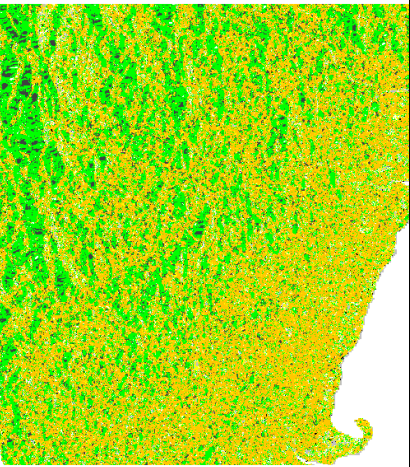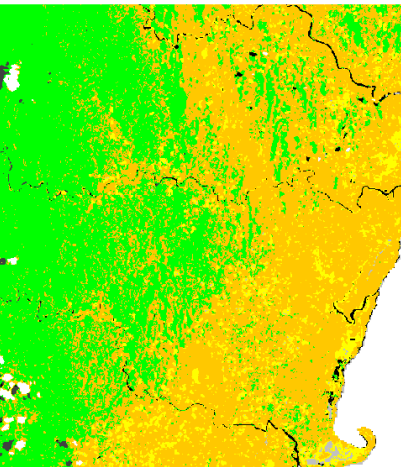
Sentinel-2 image on February 20th, 2017, in natural colors	Sentinel-1 image on February 18th, 2017 (Dual Pol Difference Sigma0 db VV + VH)	Fused image resulting from the combination of the Sentinel-1 and Sentinel-2 images
KNN classification of the Sentinel-2 image	KNN classification of the Sentinel-1 image	KNN classification of the fused image

Table 1. Optical, Radar and Stacked Optical and Radar Image with the Result of a KNN Classifier Applied To Each Image.

Class	Color
Non-forest vegetation	
Forest	
Water	
Ground	
Waterway	
Other	
Cloud	
Cloud shadow	

Table 2. Class Names and Colors

Future work

For the classification task different classifiers can be used including convolutional neural networks (CNN) which we propose to use in future work. With CNN we are looking to be able to achieve the classification task with minimal preprocessing and pre-defined features, relying on the CNN to extract the relevant features for each class.

To predict future deforestation events, we plan to use time series. Furthermore, by combining earth observation data with information on the area of interest with data from other sources such as research publications, social and economic indicators, demographic data, and others, it can be possible to understand the drivers of the deforestation. Additionally, ground truths can be collected on a testing site to increase the accuracy of the classification and validate the results of the predictions.

References

Hansen, M. C., Potapov, P. V., Moore, R., Hancher, M., Turubanova, S. A., Tyukavina, A., . . . Townshend, J. R. (2013). High-Resolution Global Maps of 21st-Century Forest Cover Change. *Science*, 850–854.

Use Case 7:

Global Warming Impact Assessment on the Bracciano Lake Surface Temperature

Implemented by: FabSpace Rome, Italy

Contact: Davide De Santis (*Davide.De.Santis@uniroma2.it*)

8. Use Case 7: Global Warming Impact Assessment on the Bracciano Lake Surface Temperature

Bracciano Lake, RGB L2A image from Sentinel 2A, 30th July 2017

Introduction

The last three years were the hottest on global scale since historical measurements are available. In particular, in 2016 in Italy a temperature anomaly of +1.35 °C above the mean over the period 1961-1990 has been registered (Figure 1).
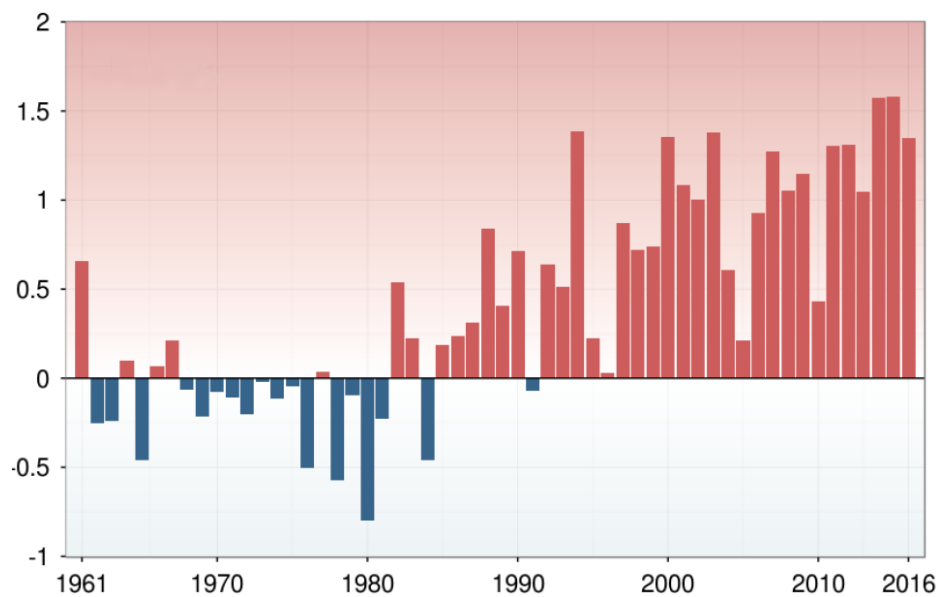
Figure 1: Mean temperature anomalies (°C) time series based over the period 1961-1990 in Italy.

On a regional scale, climate change is causing the temperature increase of coastal and inland waters. In the case of lakes, in particular, the water warming is causing rise in algal blooms frequency and in percentage of water lost through evaporation.

As result of water supply, evaporation and rainfall deficit (study area approximately -50%; -30% at national scale in 2017), the Bracciano Lake water level has suffered a critical decrease in the last three years and currently is more than 1.50 meters lower in comparison with the historical mean value for the period. This means that the whole lacustrine ecosystem is in a very unstable state of equilibrium. In August 2017, the water level was so low that when the tourist boat running from Bracciano's lakeside area to the towns of Trevignano and Anguillara was unable to operate. Since the Lake critical situation, many associations consisting in groups of stakeholders have been created. They have started to monitor the Bracciano Lake water level and ecosystem and make awareness to people and public institutions.

One of these associations, called Progetto Comune, has contacted the FabSpace of Rome about the critical water level point of the Bracciano Lake in summer 2017. In particular, they wanted to estimate the water surface temperature of the Lake and its trend in the last decade using satellite data, in order to monitor the impact of Global Warming on the Lake water. A rise in water temperature is directly correlated to the increase in water lost due to the evaporation phenomenon.

Study Area

Lake Bracciano (42.12 N, 12.23 E) is a volcanic lake located 30-km Northwest of Rome (Lazio, Italy), belonging to Sabatino Volcanic District (Figure 2).

This Lake is one of the most important natural drinking water reservoirs of the Lazio Region and it does not have a suitable network to monitor lake's parameters, such as the water temperature.
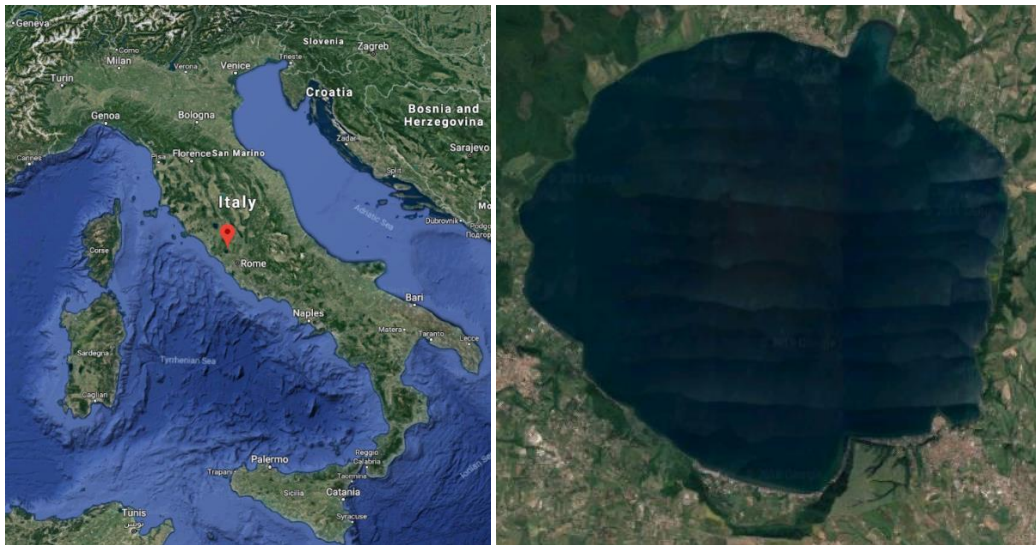
Figure 2: Study area – Bracciano Lake (Google images).

Bracciano Lake Main Features	
Maximum Depth	165.00 m
Mean Depth	88.63 m
Perimeter	31.5 km
Water Surface Area	57.02 km^2
Water Volume	5.05 km^3
Catchment Area	146.7 km^2

Bracciano Lake is a rich source of flora and fauna, including the endemic algae Isoëtes Sabatina (as far as we know, not to be found anywhere else) and plentiful stocks of fish. The Lake is characterized by a modest catchment area 147.483km2 mainly composed by 24 sub-basin with different shape and dimensions (Rossi et al., 2018), as shown in Figure 3.
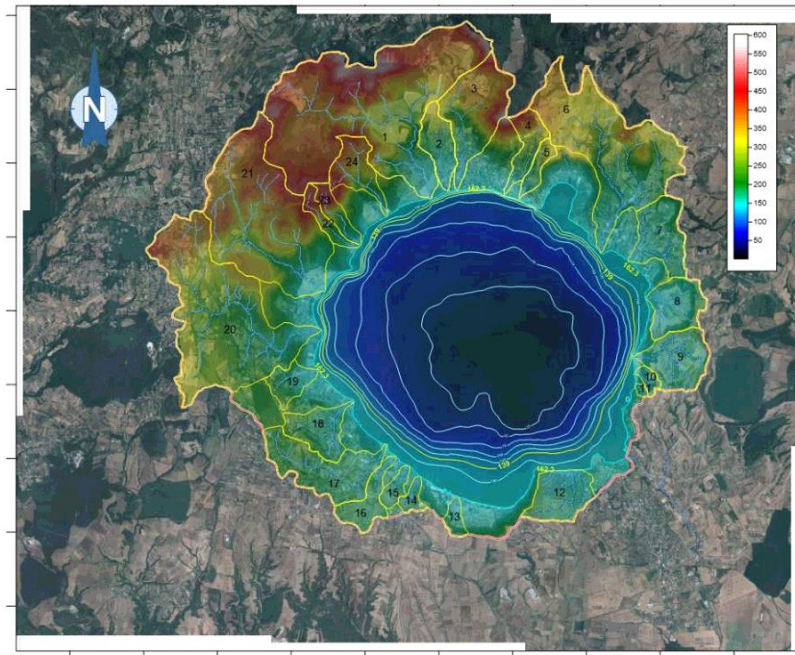
Figure 3: Bracciano Lake catchment area (Rossi et al. 2018).

As every deep lake, the Bracciano Lake is characterized by a greater thermal stratification stability in case of a water temperature increase. This phenomenon causes the depth decrease of the mixing layer and, consequently, a higher risk of eutrophication and a worsening in water quality of the Lake.

Material and Methods

In order to achieve the aim of the work, more than 200 satellite imagery have been elaborated: the data were acquired from Landsat 5, Landsat 7 and Landsat 8 from 2000 to 2017 (see the table below).

Satellite	Data	Period
Landsat 5	42	2000-2011
Landsat 7	164	2000-2017
Landsat 8	52	2013-2017

Landsat - Band	Spectral Res	Spatial Res
L5 – B6	10.4-12.5 µm	120 m
L7 – B6	10.4-12.5 µm	60 m
L8 – B10	10.6-11.2 µm	100 m

The water surface temperature has been obtained through a radiative transfer equation-based algorithm (Yu et al., 2014), according to the following steps for the images processing (De Santis and Del Frate, 2018).

1.   *Radiometric calibration*: from acquired Digital Number value to Spectral Radiance;

2.   *Atmospheric calibration*: to obtain the Spectral Radiance value atmospherically corrected;

3.   *Water surface temperature calculation.*

Results and Discussions

Implementing the shown algorithm in a GIS platform, more than 200 thermal maps of the Bracciano Lake has been obtained. As an example, the comparison between the water surface temperature in the early August in 2013 and 2017 is reported in Figure 4.
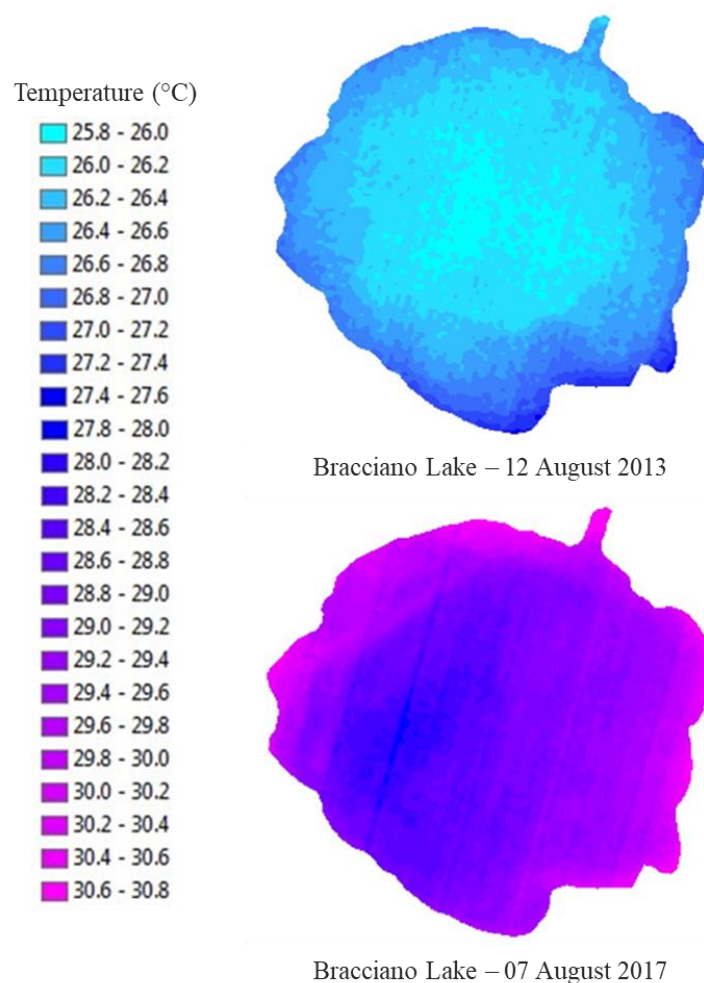
Figure 4: Water surface temperature of the Bracciano Lake from Landsat 8 (De Santis and Del Frate, 2018).

From the thermal maps, representative mean water temperature values have been estimated and then monthly averaged (see the following table) in order to compare the mean water surface temperature (WST) in different temporal ranges.

Month	Mean T (°C)	D.S. (°C)	Month	Mean T (°C)	D.S. (°C)
JAN	9.307	0.915	JUL	26.436	0.960
FEB	9.373	0.582	AUG	25.988	1.228
MAR	10.938	1.229	SEP	24.145	1.319
APR	14.407	1.270	OCT	19.998	1.666
MAY	19.409	1.086	NOV	15.773	1.536
JUN	24.213	1.059	DEC	12.665	1.079

From the obtained values has been possible to estimate that in 2017 the average temperature of the Bracciano Lake surface was 18.40 °C (+0.72 °C in comparison to the mean of the period 2000-2017). In particular, in 2017, the maximum water surface temperature was 26.86 °C in July and the minimum was 10.58 °C in February (respectively +1.32 °C and +0.51 °C in comparison to the mean of the period 2000-2017). Moreover, the comparison between the water surface temperature monthly averaged in 2010 and 2017 is reported in Figure 5.

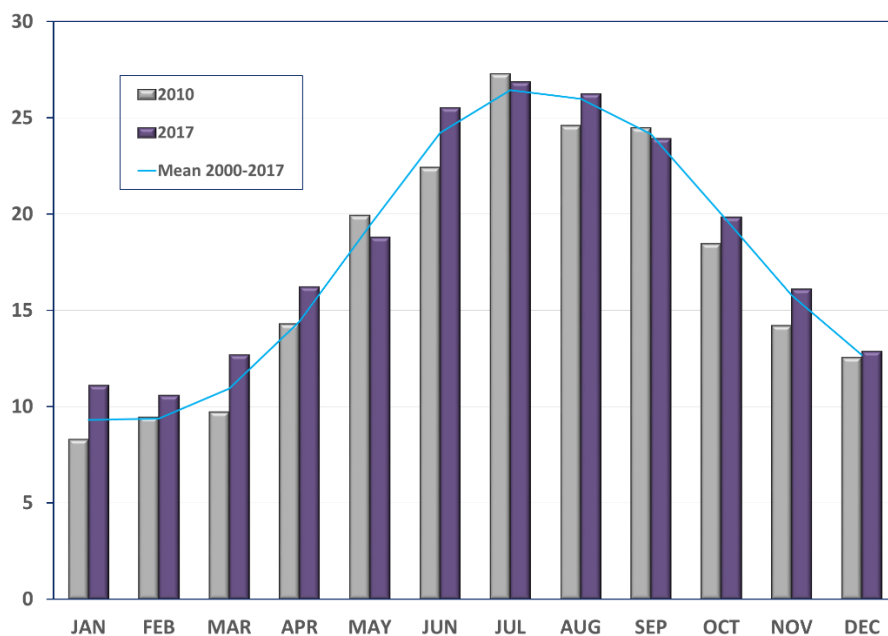Figure 5: Mean water surface temperature of the Bracciano Lake in 2010 and 2017 in comparison with the mean over the period 2000-2017 (De Santis and Del Frate, 2018).

The most part of the temporal ranges analysed (consisting of a single month or a season) have shown a general rising trend of in water surface temperature during the last decade. As an example, the trend of March, July, spring and summer are show in Figure 6.
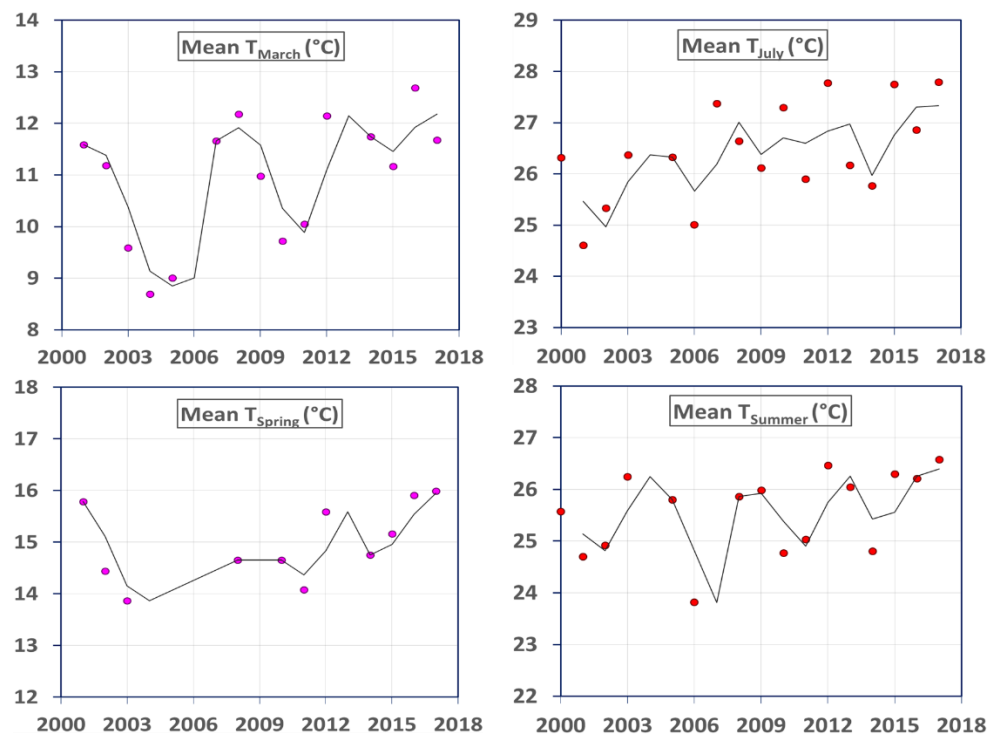
Figure 6: Monthly and seasonal mean of Water Surface Temperature (°C) trends from 2000 to 2017 of the Bracciano Lake (De Santis and Del Frate, 2018).

For a validation of the results, in addition to Bracciano Lake, the shown algorithm for the WST calculation has been tested on 100 Landsat products corresponding to five different USA lakes. The in-situ water temperature considered as ground truth are provided by NOAA choosing the appropriate measurement station at the link http://www.ndbc.noaa.gov/obs.shtml. Temperature values estimated from satellite data, in comparison with in situ recorded data, have shown a very good accuracy of the algorithm and a RMSE = 0.651 °C.

Furthermore, considering mathematical models and correlations available in literature can be retrieved the water lost percentage due to evaporation, which is rising in the last years due the Global Warming as the water temperature. A recent research over the same area assessed that the Bracciano Lake evaporation rates (Figure 7) have ranged from 6.4 to 7.3 mm/day during summer 2017, in comparison to the annual average of 3.6 mm/day over the period 2007-2017 (Rossi et al., 2018).
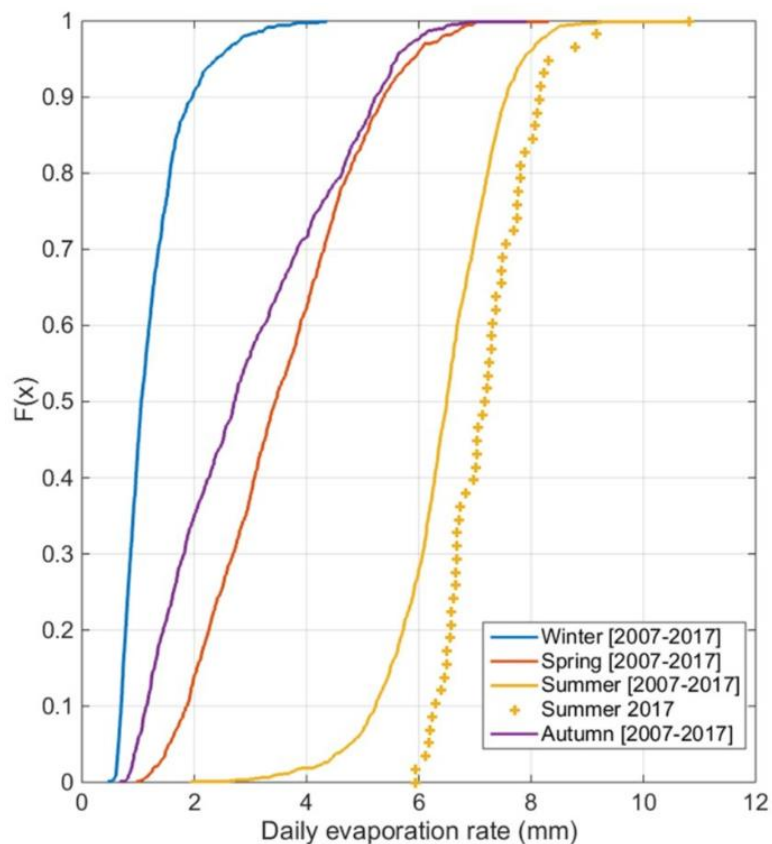
Figure 7: Bracciano Lake evaporation rate range: comparison between summer 2017 and seasonal mean over the period 2007-2017 (Rossi et al., 2018).

Conclusion

The goal of this use case was to estimate the water surface temperature of the Bracciano Lake and its trend in the last decade, in order to monitor the water warming of the Lake, which is strictly connected to the water deficit due to evaporation. Almost all the average values over the temporal ranges analysed have shown a general rising trend in water surface temperature. The estimated values from satellite data in comparison with in situ recorded data have shown a very good accuracy of the algorithm (RMSE = 0.651 °C). The water warming registered in the last years is correlated with the increase in water lost due to evaporation, which was found out in other researches.

References

D. De Santis and F. Del Frate; *Monitoring of Climate Change Effects on Water Surface Temperature of the Bracciano Lake*, Poster session at the "Mapping Water Bodies from Space 2nd Conference", Frascati (Rome) – ESA-ESRIN, 27-28 March 2018.

D. Rossi, E. Romano, N. Guyennon, S. Ghergo, D. Parrone, M. Rainaldi, A. Mecali, E. Perugini, A. Scala and S. Taviani; *Present state of Lake Bracciano: hope and despair,* Poster session at the "La previsione idrogeologica sulla risorsa acqua Conference", Rome – Accademia Nazionale dei Lincei, 22 March 2018.

X. Yu, X. Guo, Z. Wu; *Land Surface Temperature Retrieval from Landsat 8 TIRS—Comparison between Radiative Transfer Equation-Based Method, Split Window Algorithm and Single Channel Method*, Remote Sens. 2014, 6, 9829-9852.

9. Conclusion of the 1st Edition – FabSpace Use Cases Series

A number of FabSpace Use Cases (i.e. 8 cases) were successfully collected, evolving into the 1st edition of FabSpace Use Cases series from the various implementations of the project.

FabSpace aims for the use cases to showcase various ideas to use EO data and tools with the aim to attract more people from different backgrounds to generate new projects and promising business plans in the future.

Continuous improvement and more use cases would be expected in the next edition. The FabSpace 2.0 project will continue on the next edition of the use cases with more challenges and categories. The project also welcomes any organizations to be involved in the development of the use cases in order to successfully implement the project findings.

FabSpace 2.0 is the open-innovation network for geodata-driven innovation – by leveraging Space data in particular, in Universities 2.0.

Its Work programme topic addressed INSO-4-2015: Innovative schemes for open innovation and science 2.0 b) Academia- Business/Public/CSO knowledge co-creation Coordination and support action. The FabSpace 2.0 project aims at making universities open innovation centres for their region and improving their contribution to the socio-economic and environmental performance of societies.

To achieve these general objectives, the FabSpace 2.0 project offers to concentrate on one research area with high expected socio-economic impact: data-driven innovation, with a particular attention to Earth observation data.

In the six European regions covered by the consortium, partner universities work together with co-located Business Incubation Centres of the European Space Agency (ESA BICs). ESA BICs aim at inspiring entrepreneurs to turn space-connected business ideas into commercial companies, and provide technical expertise and business-development support.

This consortium, completed by TerraNIS – the French company that operates the European Group of Enterprises for a Network of Information Using Space (EUGENIUS) – and IDGEO – provisioning continuous trainings in Geomatics – and the European Business Network (EBN), will be a key success factor for the project.

In addition, FabSpace 2.0 selected 14 new FabSpaces in December 2017 located in various countries worldwide including France, Italy, Czech Republic, Spain, Lithuania, Armenia, Cyprus, The Netherlands, and Cameroon. These new FabSpaces expanded the FabSpace 2.0 network from its first founder FabSpaces in France, Belgium, Germany, Italy, Greece, and Poland. The international opening of the FabSpace 2.0 network is underway and will be extended worldwide.

This project began on March 1ˢᵗ 2016 and will last 3 years. It is under the lead of Univ. Toulouse III – Paul Sabatier (UPS).

CONNECT WITH US!

www.fabspace.eu   @FabSpaceWorld

fabspace@irit.fr   fabspaceworld

Stay in touch with us in our local FabSpaces:

FabSpace (Country & City)	Contact Person	Local Website
Armenia - Yerevan	Hrachya ASTSATRYAN (hrach@sci.am)	https://www.facebook.com/groups/FabSpace2.0Armenia/
Belgium - Liège	Murielle KIRKOVE (m.kirkove@ulg.ac.be)	http://www.csl.ulg.ac.be
Cameroon - Yaoundé	Mely Lagoute Monique (mely@eurekageo.space)	www.eurekageo.space
Cyprus - Lemesos	Professor Diofantos Gl. Hadjimitsis (d.hadjimitsis@cut.ac.cy; diofantosh@gmail.com)	http://www.cyprusremotesensing.com/
Czech Republic - Prague	František Kumhála (kumhala@tf.czu.cz); Jan Kropáček (jkropacek@fzp.czu.cz)	www.czu.cz
France - Nice	Erwan PAITEL (erwan.paitel@univ-cotedazur.fr); Marc BARRET (marc.barret@univ-cotedazur.fr); Loïc CHANVILLARD (Loic.CHANVILLARD@safecluster.com)	http://univ-cotedazur.fr/en#.WqflAma0agQ
France - Plouzané (Brest)	Marie JAGAILLE (marie.jagaille@imt-atlantique.fr)	http://bretel.eu https://twitter.com/FabSpaceBzh?lang=fr
France - Talence (Bordeaux)	Toufik AHMED (tad@labri.fr)	https://enseirb-matmeca.bordeaux-inp.fr/fr
France - Toulouse	Helbert ARENAS (Helbert.Arenas@irit.fr)	https://www.irit.fr/FabSpace/fr
Germany - Darmstadt	Md Bayzidul ISLAM (bislam@psg.tu-darmstadt.de)	www.freespacedata.de and www.myearthchallenge.de
Greece - Athens	Iosif S. PARASKEVAS (isparas@mail.ntua.gr) Charalampos MARANTOS (hmarantos@microlab.ntua.gr)	https://www.facebook.com/groups/fabspacegreece/
Italy - L'Aquila	Domenico CIMINI (nico.cimini@aquila.infn.it)	http://cetemps.aquila.infn.it/
Italy - Pavia	Fabio DELL'ACQUA (fabio.dellacqua@unipv.it)	http://tlcrs.unipv.it/
Italy - Rome	Davide DE SANTIS (Davide.De.Santis@uniroma2.it); Francesco CARBONE (francesco.carbone@geo-k.co); Miguel PENALVER (penalver@disp.uniroma2.it)	https://fabspace.dicii.uniroma2.it
Italy - Torino	Piero BOCCARDO (fpiero.boccardo@polito.it)	www.ithacaweb.org
Italy - Venezia	Stefania DE ZORZI (dezorzi@ie4st.eu)	http://www.ie4st.eu
Lithuania - Vilnius	Kestutis PAPSYS (Fabspace@chgf.vu.lt)	http://www.chgf.vu.lt; http://www.chgf.vu.lt/fabspace
Poland - Warsaw	Anna BIALCZAK (Anna.Bialczak@opegieka.pl); Paulina SCIANA (Paulina.Sciana@opegieka.pl)	http://fabspace.pl/
Spain - Castellon de la Plana	Joaquín HUERTA-GUIJARRO (huerta@uji.es); Estefanía AGUILAR-MORENO (eaguilar@uji.es)	http://geotec.uji.es http://www.uji.es
The Netherlands - Noorwijk	Dr. Alexander LOS (alexander.los@neoc.space)	www.neoc.space